

A Machine Learning Solution for Video Delivery to Mitigate Co-Tier Interference in 5G HetNets

Devanshu Anand, Mohammed Amine Togou, and Gabriel-Miro Muntean

School of Electronic Engineering, Dublin City University, Ireland

Abstract—The exponential demand for multimedia services is one reason behind the substantial growth of mobile data traffic. Video traffic patterns have significantly changed in the past two years due to the coronavirus disease (Covid-19). The worldwide pandemic has caused many individuals to work from home and use various online video platforms (e.g., Zoom, Google Meet, Microsoft Teams). As a result, overloaded macrocells are unable to ensure high Quality of Experience (QoE) to all users. Heterogeneous Networks (HetNets) consisting of small cells (femtocells) and macrocells is a promising solution to mitigate this problem. A critical challenge with the deployment of femtocells in HetNets is the interference management between Macro Base Stations (MBS), Femto Base Stations (FBS), and between FBS-FBS. Indeed, the dynamic deployment of femtocells can lead to co-tier interference. With the rolling out of the 5G mobile network, it becomes imperative for mobile operators to maintain network capacity and manage different types of interference. Machine Learning (ML) is considered as a promising solution to many challenges in 5G HetNets. In this paper, we propose a Machine Learning Interference Classification and Offloading Scheme (MLICOS) to address the problem of co-tier interference between femtocells for video delivery. Two versions of MLICOS, namely, MLICOS1 and MLICOS2, are proposed. The former uses conventional ML classifiers while the latter employs advanced ML algorithms. Both versions of MLICOS are compared with the classic Proportional Fair (PF) scheduling algorithm, Variable Radius and Proportional Fair scheduling (VR+PF) algorithm, and a Cognitive Approach (CA). The ML models are assessed based on the prediction accuracy, precision, recall and F-measure. Simulation results show that MLICOS outperforms the other schemes by providing the highest throughput and the lowest delay and packet loss ratio. A statistical analysis was also carried out to depict the degree of interference faced by users when different schemes are employed.

Index Terms- HetNets, Covid-19, Interference, Machine Learning, QoS, Statistical Visualization

I. INTRODUCTION

Recently, user demand for cellular data has surged due to the rapid increase in the number of both smart devices and mobile applications. Video streaming applications, including video on demand and live streaming, account for the majority of the mobile data traffic. According to Cisco [1], video traffic has increased at a compound rate of 26% from 2016 to 2020, and will account for 82% of all the Internet traffic by the end of 2022. As video traffic and applications are increasing exponentially, the need for good resource management is of paramount importance, especially in indoor spaces. Radio signals in indoor environments are relatively weak due to aspects such as path loss and fast fading. This determines

that sometimes the bandwidth share users get from Macro Base Stations (MBS) is insufficient to support delivery of high quality multimedia content [2]. Other times, reliable and fast delivery of multimedia content is of great significance for the service provided [3]. In general, video streaming services have high bandwidth and tight timing requirements, sometimes exceeding the network support. This calls for an efficient way to deliver videos, specific to the ultra-dense HetNets [4].

One promising solution to improve the overall network capacity is to provide 5G support as part of HetNets. HetNets consist of small cells that are deployed within the macro cell coverage area. Among the small cell solutions (i.e., femtocells, microcells, and picocells), femtocells have recently received considerable attention in the new 5G service-based architecture. Femtocells do not face any challenges related to site availability, as users install FBS themselves and use existing user broadband connections. They also introduce very little overhead on the mobile operators [5]. A femtocell provides three types of access modes to its users. The open access allows access to all user equipment (UE) with no restriction, while the closed access mode enables access only to authorized users. The hybrid access enables access to authorized UEs along with a limited number of pre-defined UEs in a prioritized manner. A femtocell helps improve the indoor radio signal quality, operates on a licensed spectrum, and provides good wireless access service.

Due to limited radio resources, a femtocell shares the same licensed range with a macrocell in the traditional cellular network, leading to signal interference. The interference between the macrocell and the femtocell is called cross-tier interference. The dynamic deployment of multiple femtocells also determines a inter-cell interference known as co-tier interference, which is one of the primary concerns with femtocell deployment in HetNets. In an ideal HetNet, co-tier interference can be minimized if femtocells are deployed with appropriate planning. However, due to the plug and play feature of femtocells, co-tier interference occurs even after appropriate planning. *In HetNets, there will always be more femtocells than macrocells. A high number of femtocells helps reduce the load of the macrocells. However, such a setup introduces interference, in particular co-tier interference and it is important to address it in order to ensure good QoS levels and high user QoE.*

All major video content providers (e.g., Youtube, Youku, Netflix) have put great efforts to deliver the most exciting

content to users [6]. They require increased amount of bandwidth and this calls for the use of femtocells in a HetNet environment. Femtocell employment results in interference, which ultimately affects the delivered content's quality of service (QoS). Therefore, there is an important need to mitigate the co-tier interference and ensure good quality of the delivered multimedia content in HetNets.

Following considerable research efforts, many schemes have been proposed to minimize the effect of co-tier interference in a HetNets, including clustering techniques, cognitive approaches, resource allocation solutions and power control techniques [7][8][9][10]. Among them, Sultan et al. [11] discussed power and radio resource management techniques to mitigate the co-tier interference in femtocells. However, their proposed scheme measured the level of interference for each femtocell only. Tian et al. [12] introduced a cognitive interference management technique for the Internet of Things (IoT) in a two-tier network. Pyun et al. [13] proposed a heuristic optimization resource allocation scheme to mitigate co-tier interference during uplink transmissions in femtocell networks. Dai et al. [14] introduced an interference management technique based on resource allocation and common clustering method in order to mitigate co-tier interference in an Orthogonal Frequency Division Multiplexing (OFDM)-based femtocell network. All the different schemes from the literature proposed good unique solutions to mitigate co-tier interference. However, as these methods cannot be used in an online mode, novel techniques are sought, including using ML [15].

This paper proposes the **Machine-Learning Interference Classification and Offloading Scheme, MLCOS**, a ML-based solution for the co-tier interference problem during video delivery in HetNets. The proposed solution involves a novel machine learning-based interference classification algorithm and an offloading scheme applied on the most affected traffic to mitigate the co-tier interference between the femtocells and improve QoS levels.

Fig 1 illustrates the two-tier HetNet environment deployment for video delivery considered in this work. It involves multiple femtocells and one macrocell. We assume femtocells employ the closed access mode. The proposed MLCOS scheme gives femtocells a cognitive sense that helps classify users based on the interference level they experience. MLCOS selects the most affected users and offloads their traffic to nearby FBS, reducing the co-tier interference and improving the overall QoS. The ML algorithms used by MLCOS are assessed in terms of prediction accuracy, precision, recall and F-measure. Two versions of MLCOS are proposed, namely, MLCOS1 and MLCOS2. MLCOS1 uses the conventional ML algorithms and MLCOS2 uses the neural network algorithms. Both versions are tested in the simulated HetNet and their performance is compared with that of other state-of-the-art solutions based on QoS metrics such as throughput, delay and Packet Loss Ratio (PLR).

The main contributions of this paper are as follows:

- 1) We propose a ML solution to address the problem of co-tier interference. The proposed solution has two stages.

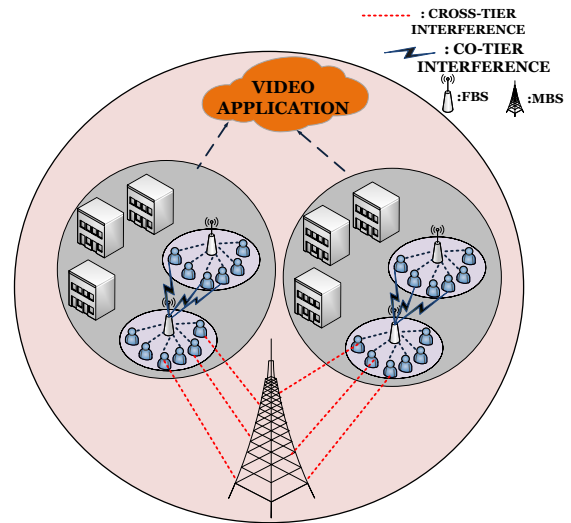


Fig. 1: An example of a two-tier HetNet, including one MBS and several FBS, located in residential buildings that constitute hotspots for wireless traffic. In this scenario, most UEs are streaming videos while the rest are generating regular web traffic. UEs in a given region are either served by MBS or FBS, which can lead to co-tier and cross-tier interference, affecting QoS and user QoE.

The first classifies the users based on the interference level while the second offloads users from the high interference class to nearby FBS.

- 2) We perform an in-depth performance analysis of the proposed versions of MLCOS against three other schemes, demonstrating the proposed solution's superiority.

The rest of the paper is organised as follows. Section II surveys some related works. Section III formulates the problem. The system model and proposed MLCOS algorithm are presented in Section IV. Performance evaluation, including ML analysis, QoS assessment and result visualization and analysis, is discussed in Section V. Finally, Section VI concludes the paper and indicates some future research directions.

II. RELATED WORKS

A HetNet may involve a large numbers of UEs and access points, making it challenging to meet the delay-sensitive QoS demands for video applications and services. In addition, the dynamic deployment of femtocells in HetNets may lead to co-tier interferences, which can reduce the overall network's capacity. There is an abundant number of interference management schemes and techniques that have been proposed in the literature. In this section, we briefly review some of the existing co-tier interference management techniques. They are organised into four different categories: clustering techniques, cognitive approaches, resource allocation schemes, and power control techniques.

A. Clustering Techniques

Clustering techniques identifies similarities between users based on vicinity, power, cell clustering policy, and groups

them according to those characteristics which are common. These groups are known as "clusters". In [16], the authors proposed a semi-clustering of victim-cell (SCVC) approach, which clusters users based on UEs status (*i.e.*, critical and non-critical), and accordingly, assigns resource blocks among the various clusters. This helps to manage the co-tier interference. In [17], the authors divided the problem into two sub-problems. First, a femtocell clustering scheme based on LINGO for mathematical modelling is used. Second, a novel algorithm is proposed to allocate sub-channels to femtocell users. The proposed algorithm predicts the change tendency of path loss values of UEs. A clustering approach that groups users and femtocells based on line of sight connectivity has been introduced in [18], while Wang *et al.* [19] proposed a Data-Driven Power Control (DDPC) technique based on affinity propagation (AP) clustering algorithm. It clusters the various femtocells based on the reference signal received power (RSRP). In [20], the authors have proposed a dynamic cell clustering-based resource algorithm to mitigate the co-tier interference in the femtocells. The proposed algorithm includes two steps, one for assigning sub-channels for users and the second helps mitigate the interference by controlling the power. In [21], the authors proposed a small cell power control algorithm (SPC) and interference-managed hybrid clustering (IMHC) scheme, to resolve the issue of co-tier and cross-tier interference in the small cell base station cluster tiers. The proposed scheme improved the system throughput with reduced interference but did not consider other QoS metrics like jitter, PLR and delay. In [22], the authors proposed an interference management technique to mitigate the problem of co-tier interference in ultra-dense small cell networks. It deploys a clustering based interference management scheme in which the sub-channel resources are allocated in the process of cluster generation. While clustering techniques find common characteristics and group users into different clusters, classification algorithms use pre-defined classes to which users are assigned.

B. Cognitive Approaches

Cognitive Approaches have been proposed for a long time in literature to mitigate co-tier interference. Tian *et al.* [12] proposed a cognitive technique for a network of femtocells serving multiple IoT devices. The authors described two cognitive Interference Alignment (IA) schemes. The first offers a nulling based IA scheme that aligns the co-tier interferences into the orthogonal subspace at each IoT receiver. The second presents a partial cognitive IA scheme that further enhances the network performance with low Signal to Noise Ratio values. Zhang *et al.* [23] proposed a cognitive approach to mitigate co-tier interference in femtocells. In the proposed scheme, a FBS allocates component carriers to its UE for transmission. The UE uses RSRP values to perform path loss measurements from its FBS and neighbouring FBS. If the RSRP value is low on one of the component carriers, the FBS selects that component carrier as primary to help reducing the co-tier interference. Similarly, a Cognitive Radio Femtocell Base Station (CFBS) is

proposed in [24]. The CFBS constructs the radio environment map (REM) by sensing the radio environment. The REM is used to assign resources to authorized users and therefore helps mitigate interference. A dynamic algorithm based on distance-based approach is proposed in [25]. It minimizes the interference in a Device-to-Device (D2D) enabled cellular network and guarantees QoS for both cellular and D2D communication links. Finally, Wang *et al.* [26] used a cognitive relay to increase the capacity of femtocell users and avoid co-tier interference among femtocells.

C. Resource Allocation

Resource allocation techniques basically help allocate resources in an efficient manner in HetNets, along with reducing the co-tier interference. In [27], the authors proposed a statistical resource allocation scheme that helps mitigate the cross-tier, co-tier and cross-link interferences in ultra-dense heterogeneous networks. They consider Time Division Duplex (TDD) mode for uplink and downlink transmission, which can lead to cross-slot interference. This can be avoided by using the Frequency Division Duplex (FDD) mode. In [28], the authors proposed a Variable Radius algorithm for enhanced distribution of resources and Interference management in a LTE Femtocell network. The scenario considered the femtocell's open access mode, where all users are authorized to connect to the femtocell network. In [29], the authors described a bat algorithm based on the nearest-integer discretization method to minimize the interference in a closed access femtocell network. In [30], the authors analyzed the issue of resource allocation in 5G networks by classifying the various proposed resource allocation schemes and assessing their ability to enhance service quality. In [31], the authors considered the hybrid access mode in a FBS deployment scenario and proposed a resource allocation technique based on a cuckoo search algorithm RACSA for cross-tier interference mitigation in Orthogonal Frequency Division Multiple Access-based Long Term Evolution (OFDMA-LTE) system.

D. Power Control Techniques

Chen *et al.* [32] proposed a threshold-based handover algorithm to mitigate co-channel interference in a two-tier femtocell network. The proposed scheme considers a Signal to Interference and Noise Ratio (SINR) value as the threshold to manage the transmission power of the FBS. Unfortunately, only the uplink co-channel interference was considered. In [33], the authors proposed two power control methods to reduce the interference effect in a two-tier network using SINR. Both methods were able to mitigate well the impact of interference by controlling the transmission power. An Active Power Control (APC) technique was proposed in [34] which helps to reduce the inter-cell interference and also reduces wastage of unnecessary power consumption in a green femtocell network. In [35], the authors proposed a soft frequency reuse (SFR) scheme to minimize the interference and increase the network throughput. The proposed scheme solves the interference problem of the densely deployed SCs

by dividing the cell region into center and edge zones. The proposed scheme is based on on/off switching which tackles the elevated power consumption problem and enhances the power efficiency of 5G networks. In [36], Stackelberg game theory was used to formulate a power control scheme that mitigates interference in a shared spectrum two-tier network. The proposed scheme was compared with the baseline scheme, where a two-way pricing mechanism was integrated into the Stackelberg game to reduce the co-tier interference among femtocells.

The schemes mentioned from the research literature help mitigate co-tier interference among femtocells. To the best of our knowledge, no ML-based solution has been proposed to assess the level of interference faced by users when delivering multimedia content and address co-tier interference problem in a 5G HetNets. This paper proposes such a scheme which considers video content to be delivered among the femtocell users and mitigate the co-tier interference which impacts the video delivery content by making efficient use of resources while maintaining high QoS values in a 5G HetNets.

III. PROBLEM FORMULATION

We consider a heterogeneous network environment consisting of a set of MBSs $M = \{M_1, M_2, M_3, \dots, M_m, \dots, M_{N_m}\}$ and a set of FBSs $F = \{F_1, F_2, F_3, \dots, F_f, \dots, F_{N_f}\}$, within the coverage area of the MBSs. A simplified version of the network scenario with a single MBS is illustrated in Fig 1. We assume that users are randomly allocated to the nearest FBS. Let U denote a set of UEs which are randomly and uniformly distributed: $U = \{u_1, u_2, u_3, \dots, u_i, \dots, u_{N_u}\}$.

The communication quality in the context of existing interference between user u_i and F_f , in the coverage area of M_m , is measured by $\alpha_{i,f}$, computed as follows:

$$\alpha_{i,f} = \frac{P_i^f G_i^f}{N_o^2 + \sum_{u_j \in U} P_j^m G_j^m + \sum_{u_j \in U} P_j^f G_j^f} \quad (1)$$

where P_i^f and P_j^m denote the transmission power of UEs relative to F_f and M_m , respectively. G_i^f denotes the gain of the channel between u_i and the allocated F_f while G_j^m designates the gain of the channel between u_j and the allocated M_m . N_o is the channel's average white noise power. Similarly, the communication quality in the presence of interference between user u_i and M_m is expressed as follows:

$$\alpha_{i,m} = \frac{P_i^m G_i^m}{N_o^2 + \sum_{u_j \in U} P_j^m G_j^m + \sum_{u_j \in U} P_j^f G_j^f} \quad (2)$$

The maximum achievable throughput by the network can be expressed by Shannon's Law and is given by:

$$Thr = \sum_{u_i \in U} (B_i^f \log_2(1 + \alpha_{i,f}) + B_i^m \log_2(1 + \alpha_{i,m})) \quad (3)$$

where Thr is the sum of throughput in the network, B_i^f and B_i^m are the bandwidths available for user u_i when associated with FBS F_f and MBS M_m , respectively.

The total round trip delay experienced by a packet exchanged between user u_i and FBS F_f can be expressed as follows:

$$D_{i,f} = D_{i,f}^t + D_{i,f}^{pr} + D_{i,f}^p + D_{i,f}^q \quad (4)$$

where, $D_{i,f}^t$ is the transmission delay, defined as the time it takes to transmit packets; $D_{i,f}^{pr}$ is the radio propagation delay, described as the time packets take to reach the receiver; $D_{i,f}^p$ is the signal processing delay, indicating the time to decode the packet at the receiver while $D_{i,f}^q$ is the queuing delay, specifying the packet waiting time in the buffer. If we assume that the radio propagation delay and signal processing delay are very small [37] and are negligible, the total round trip packet delay can be expressed as:

$$D_{i,f} = D_{i,f}^t + D_{i,f}^q \quad (5)$$

Similarly, the round trip delay experienced by a packet exchanged between u_i and MBS M_m can be computed as:

$$D_{i,m} = D_{i,m}^t + D_{i,m}^q \quad (6)$$

Thus, the mean delay values for user u_i are:

$$\bar{D}_{i,f} = \sum D_{i,f} / N_{i,f} \quad (7)$$

$$\bar{D}_{i,m} = \sum D_{i,m} / N_{i,m} \quad (8)$$

where $N_{i,f}$ and $N_{i,m}$ are numbers of delay samples.

Assuming that loss is a random process that follows a Bernoulli distribution [38], [39], [40], the Packet Loss Rate (PLR) between FBS F_f and u_i is expressed as:

$$\sigma_{i,f} = \sqrt{X_{i,f} * Y_{i,f} / N_{i,f}} \quad (9)$$

where $X_{i,f}$ is the probability of dropping a packet, $Y_{i,f}$ is the probability of receiving a packet (can also be expressed as $(1 - X_{i,f})$) and $N_{i,f}$ is the total number of samples. Likewise, PLR between MBS M_m and u_i is expressed as:

$$\sigma_{i,m} = \sqrt{X_{i,m} * Y_{i,m} / N_{i,m}} \quad (10)$$

The problem described in this work has three goals: G_1, G_2, G_3 , expressed in terms of the following equations:

- 1) Maximize the network throughput, calculated according to Eq. (3):

$$G_1 = \max(Thr) \quad (11)$$

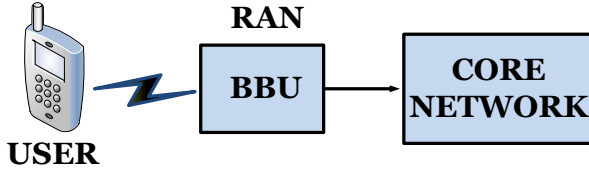
- 2) Minimize average packet delay across all users (calculated according to Eqs. (7) and (8):

$$G_2 = \min \left(\left[\sum_{u_i \in U} \bar{D}_{i,f} + \sum_{u_i \in U} \bar{D}_{i,m} \right] / N_u \right) \quad (12)$$

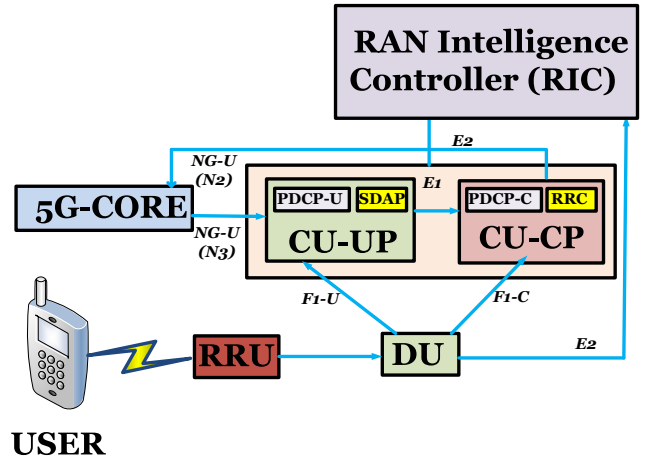
- 3) Minimize average PLR across all users (calculated according to Eqs. (9) and (10):

$$G_3 = \min \left(\left[\sum_{u_i \in U} \sigma_{i,f} + \sum_{u_i \in U} \sigma_{i,m} \right] / N_u \right) \quad (13)$$

These goals are achieved by reducing the co-tier interference in the femtocell-enhanced network environment, therefore, improving the quality of the multimedia content delivery.



(a) Traditional Radio Access Network (RAN) Architecture



(b) O-RAN System Architecture

Fig. 2: RAN network supported in traditional 3G/4G and new 5G cellular network

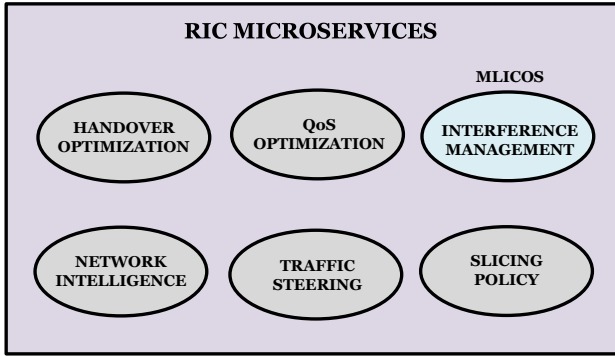


Fig. 3: MLICOS interference management service as part of the RIC microservices

IV. SYSTEM MODEL

A. System Architecture

This paper considers an Open-Radio Access Network (O-RAN) architecture, supported in a 5G network environment [41]. Within the O-RAN architecture, the functions of the traditional RAN are split into multiple entities with open interfaces between them: Remote Radio Unit (RRU), Distributed Unit (DU) and Centralised Unit (CU). These entities can be developed by different vendors, allowing for flexibility.

Fig 2a illustrates RAN components in a traditional network context. The traditional RAN network is considered a black box in which the internal interfaces are closed and operated only by a single vendor. Fig 2b shows the O-RAN-enhanced system architecture. According to the 3GPP standards, CU consists of a logical unit that integrates the Radio Resource Control (RRC), Service Data Adaptation Protocol (SDAP) and Packet Data Convergence Protocol (PDCP). These are a part of both the User Plane (UP) and the Control Plane (CP). CP carries the signalling traffic and UP transports the user traffic. CU also controls the operations of one or multiple DUs, which are logical units that host Radio Link Control

(RLC), Medium Access Control (MAC), and are partially controlled by CU. RRU is integrated with the 5G MIMO antenna [42]. An essential part of this system architecture is the RAN Intelligence Controller (RIC), containing various artificial intelligence (AI)/ML models that help improve network operations. AI/ML models situated in the RIC controller support many microservices, including handover optimization, QoS optimization, network slicing and interference management [43]. The proposed MLICOS scheme is part of this intelligence (see Fig. 3).

As illustrated in Fig. 4, MLICOS includes an Interference Management Server (IMS) that acquires information on both co-tier and cross-tier interference in the 5G HetNets. MLICOS focuses on the co-tier interference and, as discussed, involves Classification and Traffic Offloading. Classification identifies low co-tier interference users (C-1) and high co-tier interference users (C-2). MLICOS reduces the co-tier interference for C-2 users by offloading user traffic to the nearby FBS, depending upon the availability of resources at that particular FBS. Resource monitor keeps a track of resources at a particular FBS which helps in the offloading process. Traffic offloading is performed using a solution such as the one proposed in [44].

B. Machine Learning Interference Classification and Offloading Scheme (MLICOS)

The proposed approach is a ML solution which classifies users into two different classes based on the level of experienced co-tier interference within the FBS coverage area: low co-tier interference class (C-1) and high co-tier interference class (C-2). MLICOS scheme focuses on C-2 users and offloads their traffic to a nearby FBS in order to improve QoS and QoE metrics for the video streaming services.

The proposed algorithm has three phases, as shown in Algorithm 1: *Initialization*, *Classification*, and *Offloading*. In the *Initialization* phase, U is the set of UEs, randomly and uniformly distributed. Let B_s be the set of all base stations as $B_s = \{B_1, B_2, \dots, B_{N_m}, B_{N_m+1}, \dots, B_t, \dots, B_T\}$, where T

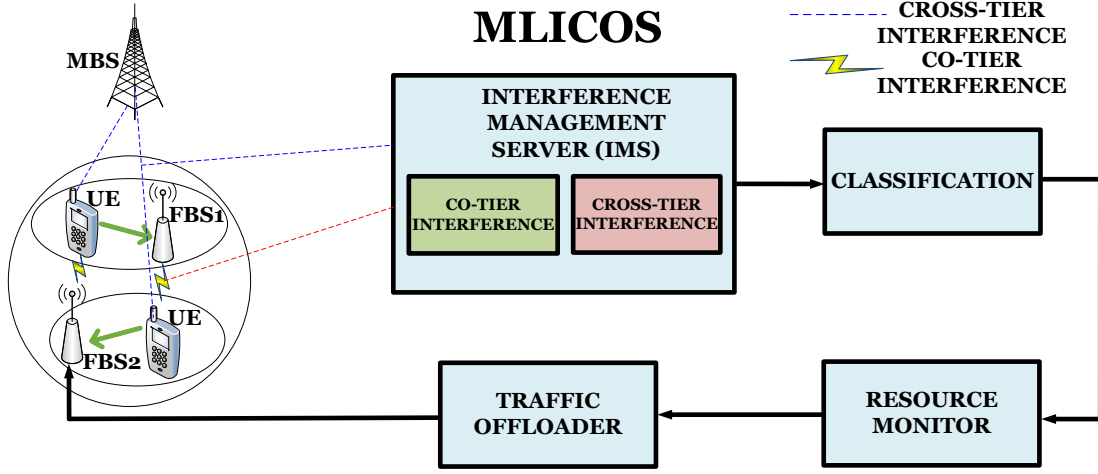


Fig. 4: MLICOS block architecture

Algorithm 1: MLICOS Algorithm

Goals: Increase Throughput (Thr), Decrease Delay (D_t) and PLR (σ)

Phase 1: Initialization :

1. $N_u, \forall u_i \in U$;
2. $C_1 = \{\}, C_2 = \{\}$;
3. $B_s = \{B_1, \dots, B_t, \dots, B_T\}$;
4. Threshold α ;
5. User Interference Matrix (UIM);
6. User Association Matrix (UAM);

Phase 2: Classification

```

foreach  $u_i \in U$  do
  foreach  $r_j^t \in N_r^t$  do
    if  $UIM[i, j] < \alpha$  then
       $C_1 \leftarrow C_1 \cup \{u_i\}$ 
      user in low co-tier interference class
    else if  $UIM[i, j] \geq \alpha$  then
       $C_2 \leftarrow C_2 \cup \{u_i\}$ 
      user in high co-tier interference class
    i++;
  end
end

```

end

Phase 3: Offloading

```

foreach  $u_i \in C_2$  AND  $B_t \in B_s$  do
  if  $UAM[i, t] = 1$  then
    Compute  $S^i$  as in eq. (16);
    Determine  $s_g^i$  as in eq. (17);
    foreach  $r_j^t \in N_r^t$  do
      Offload  $u_i$  to a new FBS  $B_g$  having the
      available resource blocks and which guarantees
      maximum throughput, lowest delay and PLR
      according to eq. (11), (12), and (13);
      Update UIM and UAM
    end
  ;
  i++;
end

```

resource blocks available at each BS $t \in B_s$ are the same. This assumption does not affect the generality of the solution. These resource blocks are further divided into sub-channels and are assigned to the UEs associated with BS_t . In the *Initialization* phase, two matrices are filled. They are defined as follows:

$$UIM = \begin{bmatrix} UIM_{1,1} & \dots & UIM_{1,N_r^t} \\ UIM_{2,1} & \dots & UIM_{2,N_r^t} \\ \vdots & \ddots & \vdots \\ UIM_{N_u,1} & \dots & UIM_{N_u,N_r^t} \end{bmatrix} \quad (14)$$

The User Interference Matrix (UIM) is introduced in Eq. (14), where $UIM[i, j]$ indicates the effect of the interference experienced by u_i on resource block r_j^t . The interference effect is assessed using SINR values, which are calculated according to Eq. (1) with $UIM[i, j] = \alpha_{i,j}$.

$$UAM = \begin{bmatrix} UAM_{1,1} & \dots & UAM_{1,B_T} \\ UAM_{2,1} & \dots & UAM_{2,B_T} \\ \vdots & \ddots & \vdots \\ UAM_{N_u,1} & \dots & UAM_{N_u,B_T} \end{bmatrix} \quad (15)$$

The User Association Matrix (UAM) is presented in Eq. (15), where $UAM[i, t]$ indicates the association of each u_i with one BS BS_t , which can be either MBS or FBS. In this paper, we consider $UAM[i, t]$ as a binary variable. If u_i is not associated with BS_t , $UAM[i, t] = 0$; otherwise, $UAM[i, t] = 1$. Since this paper focuses on co-tier interference, we consider UEs which are associated with FBSs only ($t > N_m$). Both matrices are updated after each iteration. Note that we assume that only one user is associated with one resource block per time slot in each FBS. This assumption enables the disregard of the interference between users within the same cell.

In the *Classification* phase, we categorise users based on their experienced level of interference. In this paper, two levels are considered: *high* (C_2) and *low* (C_1). We consider α as a threshold value for assessment of the interference

$= N_m + N_f$. Let R^t be the available set of resource blocks at BS_t , defined as $R^t = \{r_1^t, r_2^t, \dots, r_j^t, \dots, r_{N_r^t}^t\}$, where N_r^t is the number of resource blocks at BS_t . We assume that the

between a user and a selected FBS. Using ML algorithms, users who experience interference above the threshold value α are assigned to C-2; The rest of the users are assigned to C-1. We tune the hyper-parameters for the ML algorithms and then perform user classification. The novelty of the ML algorithms is shown in the second stage of Algorithm 1.

In the *Offloading* phase, C-2 users are offloaded to a nearby FBS that has enough resource blocks to meet the user's requirements while also contributing to the achievement of goals G1, G2, and G3. To this end, we use the received signal strength to identify the most suited FBS. We define the vector S^i as follows:

$$S^i = \{s_1^i, s_2^i, \dots, s_f^i, \dots, s_{N_f}^i\} \quad (16)$$

where s_f^i is the signal strength experienced by user u_i with respect to FBS F_f . We compute the signal strength for each C-2 user and offload the user's traffic to FBS g , which has the lowest signal strength and available resource blocks, as indicated in Eq. (17).

$$s_g^i = \min\{s_f^i | \forall f, 1 \leq f \leq N_f\} \quad (17)$$

Note that by offloading users from macrocells to nearby femtocells, more resource blocks at the level of macrocells are made available, which can be used to improve the QoS of users in C-1, and hence contributing to the realisation of G1, G2, and G3. Also note that offloading all C2 users' traffic to new FBSs does not guarantee that there will be no interference; hence, the proposed scheme runs iteratively until all UIM values drop below α or in case no improvement has been achieved in the previous iterations.

C. Machine Learning-based Algorithm

We formulate the given challenge as a ML-based problem and used the binary classification method as a solution since it requires less training time and is usually faster to converge [45]. Fig 5 illustrates the main components of the proposed solution. First, simulations are carried out using the Network Simulator NS-3. After each iteration, relevant data is saved in a Comma Separated Value (CSV) file and constitutes our simulated dataset. The reason we opted for a simulated dataset is threefold: 1) we avert from any confidentiality and privacy liability that may arise from using a real-world dataset; 2) we know the environment used for generating the dataset. Therefore, we can easily make changes to simulation parameters along with hyperparameters of the ML models [46]; and 3) the generated dataset is specific to the scenario we are examining since it solely focuses on one type of traffic (*i.e.*, video traffic). The collected data contains values of the following parameters: SINR, RSRP, Reference Signal Received Quality (RSRQ) and cell id. The CSV file is given as input to the Python environment for classification purposes. The first step is data pre-processing, required for replacing and eliminating non-numeric or symbolic features from a dataset. Next, the feature selection stage helps eliminate noise in the data and focuses only on the relevant data in a dataset. For the

ML models used by MLICOS, SINR is the target feature of interest. The data set is split into 80% training data and 20% test data, used during training and testing of our proposed solution, respectively [47].

Two versions of MLICOS were designed: MLICOS1 and MLICOS2. MLICOS1 employs supervised ML techniques, mainly Support Vector Machine (SVM) and Random Forest (RF). While SVM is one of the best classifiers and is considered a benchmark in the field of statistical learning and ML [48], RF is an ensemble learning algorithm that can ensure high accuracy while handling multiple outliers in training and test datasets. MLICOS2 deploys two neural network approaches, Artificial Neural Network (ANN) and Convolutional Neural Network (CNN) [49]. ANN and CNN used a three-layer neural network structure composed of input, hidden and output layers. We employed the Rectified Linear Activation Function (ReLU) for training the hidden layers of the neural networks. ReLU prevents an exponential growth in the computation required to operate the neural networks. As we formulated the given problem as a binary classification problem, we used the Sigmoid (Logistic) activation function for the output layer. Both neural network models are trained from scratch. We used the Stochastic Gradient Descent (SGD) optimization algorithm for training the neural network models and applied a binary cross-entropy loss. Our solution was implemented using the Keras library in Python. We used the GridSearchCV class from the scikit-learn Python library. GridSearchCV enabled selection of the best parameters from a hyperparameter set during training [50]. The learning parameters used for the proposed scheme MLICOS2 are batch size, learning rate, number of epochs and momentum. We have trained our neural network models for 250 epochs with a learning rate of 0.1. We used a mini batch of 256 and 0.9 as momentum.

We set α as the threshold value for both MLICOS1 and MLICOS2. After the testing phase, the algorithm outputs the classes of users (C-1 and C-2) and the associated SINR values for each user. The simulations in NS-3 are performed until there are no users affected by the interference (*i.e.*, in the C-2 class) or no significant improvements have been achieved in the past iterations (*i.e.*, the number of users in the C-2 class remained the same).

V. PERFORMANCE EVALUATION

We consider a heterogeneous scenario with one MBS ($N_m = 1$) and two FBS ($N_f = 2$) along with a number of users N_u which increases linearly from 50 to 130. The Gercom's Evalvid model in NS-3 is used for video transmissions. The Evalvid model transmits the video in the form of a trace file. The sender and receiver trace files are compared, allowing for the recreation of the video at the receiver end [?]. A H.264 encoded video consisting of 300 frames with a data rate of 1200Kbps and frame rate of 30 fps was selected for streaming. Table II presents additional video stream details.

All the users are randomly allocated to the nearest FBS within the MBS coverage area. Any user between the two FBS

Network Simulator NS3

Python Environment for ML Models

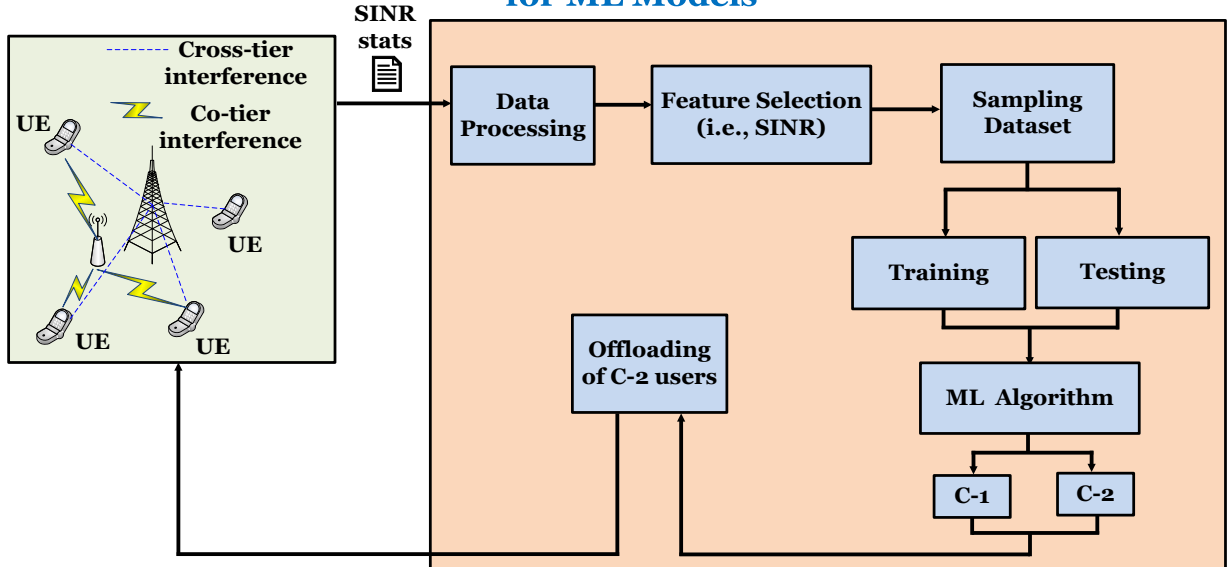


Fig. 5: Various elements of data simulation, ML algorithms, and network process

TABLE I: Simulation Parameters

Parameter	Value
Number of MBS	1
Number of FBS	2
Femtocell Coverage	10m
Max. MBS Transmit Power	46 dbm
Max. FBS Transmit Power	20 dbm
Downlink Frequency	2150 MHz
Uplink Frequency	1940 MHz
Width of Band	90 MHz
Duplex Spacing	190 MHz
Number of Resource Blocks	100
Number of Subchannels	1200
Subcarrier Bandwidth	15 KHz
Mobility Model	Constant Position
Femtocell Access	Closed Access

TABLE II: Properties for the Video Used for Transmission

Parameter	Value
Width	1280
Height	720
Total Bitrate	1209Kbps
Frame Rate	30 fps
Total Duration	10 seconds
Total Frames	300 frames

and MBS is subjected to strong interference. The macrocell also transmits signals in the same channel within the same area, resulting in interference. In this work, we consider only the co-tier interference between the femtocells and their associated users according to Eq. (1). Table I depicts the simulation parameters used.

The performance of the proposed scheme employing SVM and RF classifiers in turn is assessed in terms of accuracy, precision, recall and F-measure. The proposed scheme is

also assessed in terms of the following QoS parameters: throughput, PLR and delay.

A. MLCOS Classifier Assessment

The classifier assessment is evaluated based on the following metrics:

1) *Accuracy*: defined as the percentage of correctly classified predictions (CP), divided by total number of predictions (T) made by a model in a dataset.

$$Accuracy = \frac{CP}{T} \quad (18)$$

where CP and T are defined as:

$$CP = TP + TN \quad (19)$$

$$T = TP + TN + FP + FN \quad (20)$$

where TP stands for True Positive, FP means False Positive, TN represents True Negative and FN is False Negative. TP and TN correctly indicates the presence or absence of some characteristics, whereas FP and FN wrongly identify the presence or absence of the same characteristics, respectively. In this paper, the characteristics are the interference levels and TP , FP , TN and FN are computed based on correct and incorrect classification of a user based on interference level when comparing the model prediction with the actual classification values.

Fig 6a depicts the accuracy for MLCOS employing SVM, RF, ANN, and CNN, respectively. We observe that **CNN achieves the highest accuracy (99.02%), followed by RF (98.91%), ANN (96.38%), and SVM (95.47%)**.

TABLE III: Machine Learning Model vs Performance Metrics

Model	Accuracy	Recall	Precision	F-measure
SVM	95.47%	91.63%	93.24%	92.42%
RF	98.91%	98.04%	97.56%	97.79%
ANN	96.38%	95.82%	96.27%	96.04%
CNN	99.02%	99.11%	98.63%	98.86%

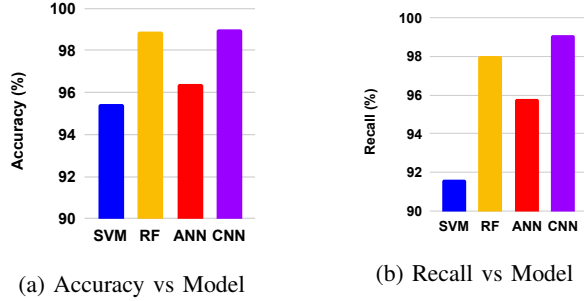


Fig. 6: Accuracy and Recall

2) *Recall*: defined as the percentage of TP predictions by the total number of actual positive predictions $TP+FN$.

$$Recall = \frac{TP}{TP + FN} \quad (21)$$

Fig 6b illustrates the recall in terms of percentage for MLICOS employing SVM, RF, ANN, and CNN, in turn. We observe that **CNN provides the highest recall (99.11%), followed by RF (98.04%), ANN (95.82%), and SVM (91.63%).**

3) *Precision*: defined as the percentage of TP predictions by the total number of positive predictions $TP+FP$.

$$Precision = \frac{TP}{TP + FP} \quad (22)$$

The precision for MLICOS employing SVM, RF, ANN, and CNN is shown in Fig 7a. **We observe that CNN achieves the highest precision (98.63%), followed by RF (97.56%), ANN (96.27%), and SVM (93.24%).**

4) *F-Measure (FM)*: defined as the harmonic mean of precision and recall and is given by:

$$FM = 2 * \frac{Precision * Recall}{Precision + Recall} \quad (23)$$

Fig 7b shows the F-measure for the four classifier models used in the proposed MLICOS algorithm. **We observe that when CNN is employed, the results include the highest F score (98.86%), followed by the scenario when in turn RF (97.79%), ANN (96.04%), and SVM (92.42%) are used respectively.** Table III summarizes the assessment results. We propose two versions of MLICOS, namely, **MLICOS1** and **MLICOS2**. The former uses SVM and RF as classification models while the latter uses ANN and CNN. Based on the superior performance results achieved and presented in Table III, the RF-based MLICOS1 and the CNN-based MLICOS2 were selected to be compared in the testing phase.

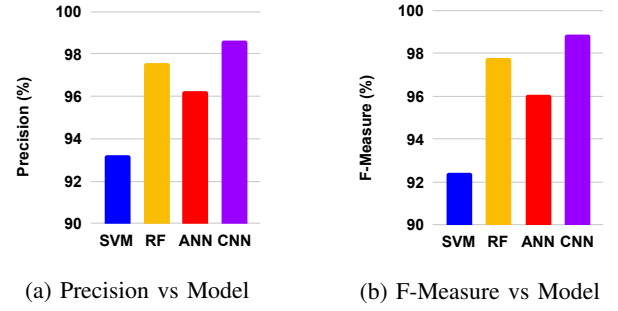


Fig. 7: Precision and F-Measure

B. QoS Assessment

When testing the performance of MLICOS1 and MLICOS2 was compared with that of the Proportional Fair (PF), Variable Radius + Proportional Fair (VR+PF) [28], and a Cognitive Approach (CA) [23]. The performance was assessed in terms of QoS parameters throughput, delay and PLR.

Fig 8 illustrates the average throughput with respect to the number of users for the three schemes. For instance, MLICOS1 using RF achieved an average throughput of 6500 Kbps per user which is **83.88%, 66.79% and 41.52%** higher than the values outputted by PF, VR + PF, and CA schemes, respectively. On the other hand, using CNN-based MLICOS2, the achieved average throughput is 6900 Kbps per user which is **84.61%, 68.28%, 44.15% and 4.51%** higher than the throughput recorded when PF, VR + PF, CA and MLICOS1 schemes are employed, respectively.

Fig 9 depicts PLR as a function of the number of users. We observe that PLR per user remains under 6% when using both MLICOS1 and MLICOS2. The value obtained by MLICOS1 is **96.912%, 87.69%, and 63.22%** lower than the results of PF, VR + PF, and CA, respectively. The value obtained using MLICOS2 scheme is **97.01%, 88.21%, 64.13% and 9.97%** lower than the results recorded when employing PF, VR+PF, CA, and MLICOS1, respectively.

Fig 10 shows the delay with respect to the number of users. Using MLICOS1, the average delay per user is less than 110 ms, compared to larger values achieved by the PF, VR + PF, and CA schemes. The value obtained is **88.73%, 78.68%, and 46.17%** lower than the delay incurred by PF, VR + PF, and CA, respectively. With MLICOS2, the average delay per user is less than 100 ms, much shorter than the large delay values achieved by PF, VR + PF, CA, and MLICOS1. The value obtained is **90.25%, 80.04%, 47.68% and 10.68%** lower than the results of PF, VR+PF, CA, and MLICOS1, respectively.

Based on the above QoS results, MLICOS2 performs better than the MLICOS1. Hence, MLICOS2 can be used in a real-world scenario with high dimension datasets and can perform better than other classification models in terms of accuracy, precision, recall and F-measure. Our simulation results show that the goals described in Eqs. (11), (12), and (13) are achieved by the proposed solution. Table IV presents a summary of the QoS results when using MLICOS1 and MLICOS2 along with three other solutions.

TABLE IV: Comparison between QoS results when using PF, VR+PF, CA and MLICOS (both versions) schemes

Users	Scheme	Throughput (Kbps)	Delay (ms)	PLR (%)
50	PF	3974.54	440.38	39.61
	VR+PF	5951.78	327.51	22.37
	CA	6757.14	106.47	16.44
	MLICOS1	7859.65	10.742	0.15
	MLICOS2	8017.68	9.82	0.12
70	PF	3765.20	558.72	65.55
	VR+PF	5514.54	401.57	48.91
	CA	6385.51	125.86	39.72
	MLICOS1	7504.77	33.43	0.72
	MLICOS2	7781.24	29.57	0.57
90	PF	2282.66	681.71	78.66
	VR+PF	4879.23	498.67	62.63
	CA	5417.71	161.55	58.2
	MLICOS1	7115.92	58.15	1.21
	MLICOS2	7369.66	52.14	0.82
110	PF	2041.24	954.1	87.66
	VR+PF	3597.72	513.56	78.711
	CA	4971.89	214.62	71.56
	MLICOS1	6904.88	75.41	4.97
	MLICOS2	7018.52	70.93	3.75
130	PF	1050.78	1029.58	98.57
	VR+PF	2165.68	647.01	89.27
	CA	3813.64	302.42	82.92
	MLICOS1	6521.54	105.94	5.53
	MLICOS2	6828.92	96.58	4.38

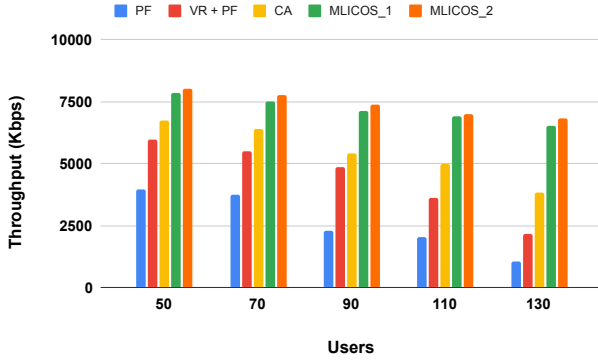


Fig. 8: Throughput vs. Number of users

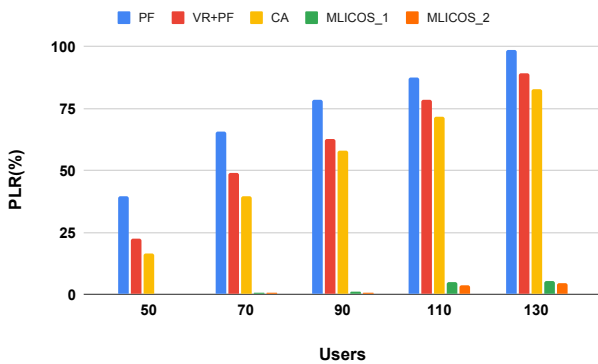


Fig. 9: PLR vs. Number of users

C. QoE Estimation

As illustrated in Fig. 1, we consider video streaming as a high priority service for users. Thus, objective quality assessment of video sequences (as perceived by a user) becomes crucial. We consider Peak signal-to-noise-ratio (PSNR) as an estimation metric for QoE. It is a signal quality metric that

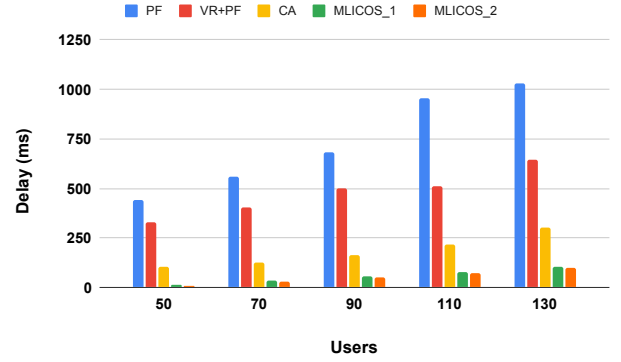


Fig. 10: Delay vs. Number of users

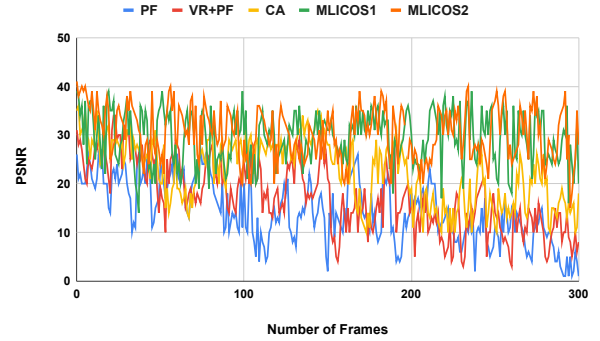


Fig. 11: PSNR Estimation

is computed over all the pixels in the video with respect to a reference video [?]. PSNR value is calculated and mapped directly on the Mean Opinion Score (MOS), as specified in ITU-T J.144 standard. The PSNR estimation outcomes are shown in Fig. 11 over 300 frames for 130 users. As can be seen, PSNR profiles are different for all the five schemes, and the perceived quality experienced by C-2 users is much better under both versions of MLICOS. Fig. 12 shows the error bar which uses standard deviation as one of the uncertainties over the mean of PSNR achieved when different schemes are used. We observe that while incurring low variations, the mean value of PSNR under MLICOS2 is **52.7%**, **42.96%**, **26.2%** and **3.3%** higher and incur much lower variations than what was achieved when the PF, VR+PF, CA, and MLICOS1 were employed, while incurring much lower variations. The numerical results show how MLICOS2 improves the user's QoE in terms of PSNR, outperforming the other schemes.

D. Statistical Visualization

To visualize the degree of interference faced by a user under all schemes, we used the Box plot (data analysis) method in R. Using this method, we can easily compare the different schemes in terms of the degree of interference experienced by C-2 users. The UIM values (according to Eq. (14) are normalized using the min-max normalization method.

Figs. 13a, 13b, 13c, 13d and 13e show the box plots for PF, VR + PF, CA, MLICOS1 and MLICOS2. The degree of interference is indicated by values ranging between 0 and 1. When values are closer to 1, they imply that users experience high co-tier interference, whereas when values are near to 0,

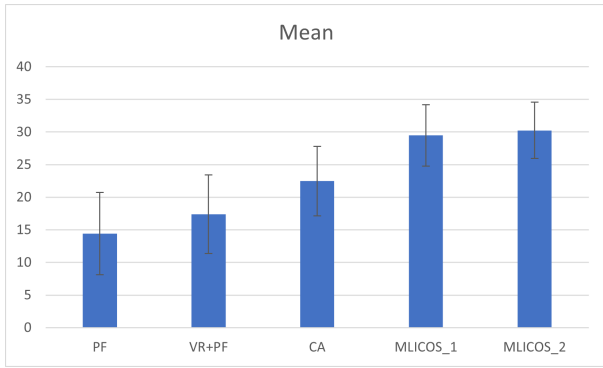


Fig. 12: Mean and Standard Deviation of PSNR

they indicate that users are the least affected by the co-tier interference.

Fig. 13a shows that when the PF scheme is applied for 50 users, most of the users face very little interference, but when the number of users increased to 130, the normalized interference value for each user is very close to 1, and almost all users are affected by co-tier interference. Fig. 13b depicts the box plot visualization for the VR + PF scheme. The box plot results of the VR + PF scheme are better than those of the PF scheme. Indeed, when the number of users is below 90, most of the users experience low co-tier interference. Still, when the number of users increases to 130, most of the users experience high co-tier interference. Fig. 13c shows the box plot for the CA scheme. When the CA scheme is deployed, we observe that when the number of users reaches 130, only 50% of users are affected by high co-tier interference. Figs. 13d and 13e illustrate the box plot for MLICOS1 and MLICOS2. We observe that users hardly experience any interference. Indeed, even when the number of users reaches 130, a tiny percentage of users experienced co-tier interference. This indicates that both versions of MLICOS maintain good QoS levels and mitigate the co-tier interference by making efficient use of resource blocks.

E. Statistical Analysis

Fig. 14 shows a direct comparison between the variability of the different schemes in terms of mean, median, maximum value and standard deviation. In relation to measuring the degree of interference, we have shown in the above section that the normalized values decide whether the user experiences high or low co-tier interference. Fig. 14 illustrates the maximum value for all schemes. In the case of PF, when there are 130 users, the ultimate value a user gets is around 0.98, which is very close to 1, and most of the users experience high co-tier interference. The VR+PF scheme performs better than the PF scheme. When 130 users are considered, the maximum value any user faces is around 0.78 and the users experience high co-tier interference. For 130 users, the CA scheme gives the maximum value of 0.49, which shows that 50% of the users are still affected by high co-tier interference. MLICOS1 incurs a maximum value of around 0.07 whereas MLICOS2 has a value of 0.05, which is very close to 0. The medians for PF,

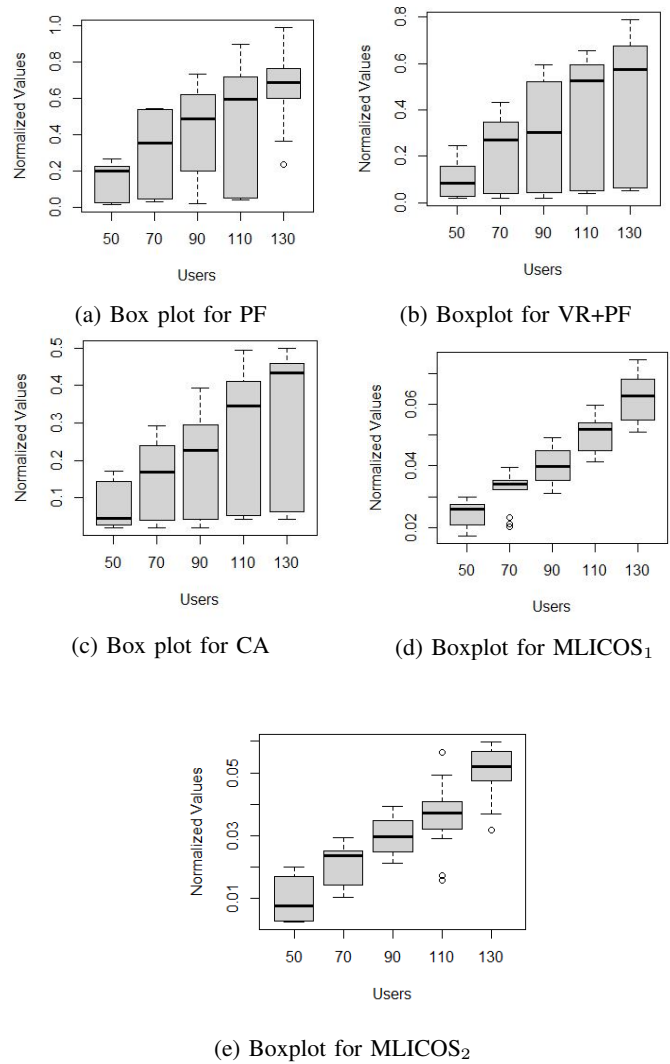


Fig. 13: Degree of interference faced by users under various compared schemes. The Y axis shows the degree of interference normalized values (0 to 1 range).

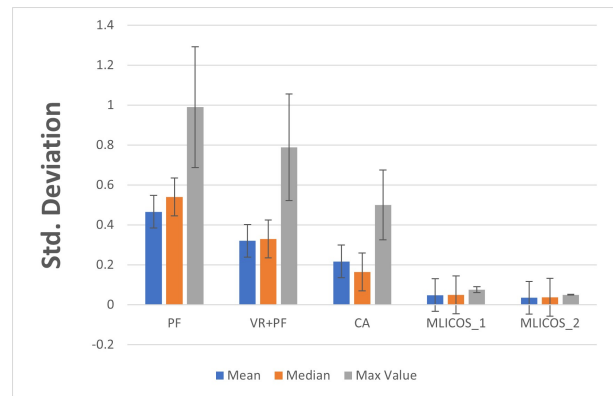


Fig. 14: Variability of different schemes

VR+PF, CA, MLICOS1, and MLICOS2 are: 0.53, 0.32, 0.16, 0.04, and 0.03, respectively. The error bar indicate how precise

TABLE V: Comparative statistical analysis of the degree of interference when different schemes are employed

Scheme	Mean	Median	Max. Value	Std. Dev
PF	0.46	0.53	0.98	0.3
VR+PF	0.31	0.32	0.78	0.26
CA	0.21	0.16	0.49	0.17
MLICOS ₁	0.047	0.049	0.07	0.01
MLICOS ₂	0.035	0.037	0.05	0.002

the measurement is or how much is the variation from the reported value. We have used standard deviation as one of the uncertainty to plot the error bars. We can conclude from Fig. 14 that both versions of MLICOS incur much lower variations and errors than those associated with the PF, VR + PF, and CA schemes. Table V summarizes the statistical analysis for all the schemes in terms of the degree of interference.

VI. CONCLUSIONS AND FUTURE WORK

In a 5G HetNet, the deployment of femtocells increases the overall network capacity. The dynamic deployment of femtocells in a HetNet leads to co-tier interference. Co-tier interference is considered as one of the significant challenges especially in urban settings. To address this problem, we proposed MLICOS, a scheme that classifies user traffic based on the interference level (*i.e.*, high and low) and offloads highly affected traffic from macrocells to nearby femtocells based on signal strength. Four ML algorithms SVM, RF, ANN and CNN are used in turn by the proposed solution for classification purposes. The performance of the ML-based algorithm is assessed in terms of prediction accuracy, precision, recall and F-measure. Based on the assessment, we propose two versions of MLICOS, MLICOS1 and MLICOS2. The former employs RF while the latter uses CNN. Both versions were compared to PF, VR + PF and CA schemes, and results show substantial improvements in terms of QoS and QoE metrics. Simulation results also show that MLICOS2 performs better than MLICOS1. Future work will define multiple user classes while also trying to consider the need for fast convergence. **Both cross-tier and co-tier interference in a HetNet will be considered in a coordinated manner in the future.**

ACKNOWLEDGEMENTS

This research was supported in part by Science Foundation Ireland under grant numbers 18/CRT/6183 (ML-LABS Centre for Research Training) and 12/RC/2289_P2 (Insight Centre for Data Analytics). For the purpose of Open Access, the author has applied a CC BY public copyright licence to any Author Accepted Manuscript version arising from this submission.

REFERENCES

[1] "Cisco annual internet report - cisco annual internet report (2018–2023) white paper," Mar 2020. [Online]. Available: <https://www.cisco.com/c/en/us/solutions/collateral/executive-perspectives/annual-internet-report/white-paper-c11-741490.html>

[2] B. Agarwal, M. A. Togou, M. Ruffini, and G.-M. Muntean, "Pirs3a: A low complexity multi-knapsack-based approach for user association and resource allocation in hetnets," in *2021 IEEE International Conference on Communications Workshops (ICC Workshops)*, 2021, pp. 1–6.

[3] P. Schulz, H. Klessig, M. Simsek, and G. Fettweis, "Modeling qoe for buffered video streaming in interference-limited cellular networks," *IEEE Transactions on Multimedia*, vol. 23, pp. 911–925, 2021.

[4] H. Zhong, F. Wu, Y. Xu, and J. Cui, "Qos-aware multicast for scalable video streaming in software-defined networks," *IEEE Transactions on Multimedia*, vol. 23, pp. 982–994, 2021.

[5] B. Agarwal, M. A. Togou, M. Ruffini, and G.-M. Muntean, "Mitigating the impact of cross-tier interference on quality in heterogeneous cellular networks," in *IEEE Conference on Local Computer Networks (LCN)*, 2020, pp. 497–502.

[6] Y. Zhou, J. Wu, T. H. Chan, S.-W. Ho, D.-M. Chiu, and D. Wu, "Interpreting video recommendation mechanisms by mining view count traces," *IEEE Transactions on Multimedia*, vol. 20, no. 8, pp. 2153–2165, 2018.

[7] G. Yang, Y. Cao, A. Esmailpour, and D. Wang, "Sdn-based hierarchical agglomerative clustering algorithm for interference mitigation in ultra-dense small cell networks," *ETRI Journal*, vol. 40, pp. 227–236, 2018.

[8] A. A. Alotaibi and M. C. Angelides, "A serious gaming approach to managing interference in ad hoc femtocell wireless networks," *Computer Communications*, vol. 134, pp. 163–184, 2019. [Online]. Available: <https://www.sciencedirect.com/science/article/pii/S0140366417309180>

[9] S. R. Samal, "Interference management techniques in small cells overlaid heterogeneous cellular networks," *J. Mobile Multimedia*, vol. 14, pp. 273–306, 2018.

[10] M. Osama, S. El Ramly, and B. Abdelhamid, "Interference mitigation and power minimization in 5g heterogeneous networks," *Electronics*, vol. 10, no. 14, 2021. [Online]. Available: <https://www.mdpi.com/2079-9292/10/14/1723>

[11] S. R. Alotaibi and H. H. Sinky, "Power and radio resource management in femtocell networks for interference mitigation," *Sensors (Basel, Switzerland)*, vol. 21, 2021.

[12] R. Tian, L. Ma, Z. Wang, and X. Tan, "Cognitive interference alignment schemes for iot oriented heterogeneous two-tier networks," *Sensors*, vol. 18, p. 2548, 08 2018.

[13] S.-Y. Pyun, W. Lee, and O. Jo, "Uplink resource allocation for interference mitigation in two-tier femtocell networks," *Mobile Information Systems*, vol. 2018, pp. 1–6, 12 2018.

[14] J. Dai and S. Wang, "Clustering-based interference management in densely deployed femtocell networks," *Digital Communications and Networks*, vol. 2, 11 2016.

[15] W. Zhu, X. Wang, and W. Gao, "Multimedia intelligence: When multimedia meets artificial intelligence," *IEEE Transactions on Multimedia*, vol. 22, no. 7, pp. 1823–1835, 2020.

[16] I. Shgluof, M. Ismail, and R. Nordin, "Semi-clustering of victim-cells approach for interference management in ultra-dense femtocell networks," *IEEE Access*, vol. 5, pp. 9032–9043, 2017.

[17] H. Zhang, D. Jiang, F. Li, K. Liu, H. Song, and H. Dai, "Cluster-based resource allocation for spectrum-sharing femtocell networks," *IEEE Access*, vol. 4, pp. 8643–8656, 2016.

[18] B. Soleimani and M. Sabbaghian, "Cluster-based resource allocation and user association in mmwave femtocell networks," *IEEE Transactions on Communications*, vol. 68, no. 3, pp. 1746–1759, 2020.

[19] L.-C. Wang, S.-H. Cheng, and A.-H. Tsai, "Data-driven power control of ultra-dense femtocells: A clustering based approach," in *26th Wireless and Optical Communication Conference (WOCC)*, 2017, pp. 1–6.

[20] D. Teng and N. Ye, "Cell clustering-based resource allocation in ultra-dense networks," in *2017 3rd IEEE International Conference on Computer and Communications (ICCC)*, 2017, pp. 622–627.

[21] N. Farhan and S. Rizvi, "An interference-managed hybrid clustering algorithm to improve system throughput," *Sensors*, vol. 22, no. 4, 2022. [Online]. Available: <https://www.mdpi.com/1424-8220/22/4/1598>

[22] G. Yang, A. Esmailpour, N. Nasser, G. Chen, Q. Liu, and P. Bai, "A hierarchical clustering algorithm for interference management in ultra-dense small cell networks," *IEEE Access*, vol. 8, pp. 78726–78736, 2020.

[23] L. Zhang, L. Yang, and T. Yang, "Cognitive interference management for lte-a femtocells with distributed carrier selection," in *2010 IEEE 72nd Vehicular Technology Conference - Fall*, 2010, pp. 1–5.

[24] G. Gür, S. Bayhan, and F. Alagöz, "Cognitive femtocell networks: an overlay architecture for localized dynamic spectrum access [dynamic spectrum management]," *IEEE Wireless Communications*, vol. 17, no. 4, pp. 62–70, 2010.

[25] M. Kamruzzaman, N. I. Sarkar, and J. Gutierrez, "A dynamic algorithm for interference management in d2d-enabled heterogeneous cellular

- networks: Modeling and analysis,” *Sensors*, vol. 22, no. 3, 2022. [Online]. Available: <https://www.mdpi.com/1424-8220/22/3/1063>
- [26] W. Wang, G. Yu, and A. Huang, “Cognitive radio enhanced interference coordination for femtocell networks,” *IEEE Communications Magazine*, vol. 51, no. 6, pp. 37–43, 2013.
- [27] F. Liu and S. Zhao, “Statistical resource allocation based on cognitive interference estimation in ultra-dense hetnets,” *IEEE Access*, vol. 8, pp. 72 548–72 557, 2020.
- [28] V. Sathya, H. V. Gudivada, H. Narayanam, B. M. Krishna, and B. R. Tamma, “Enhanced distributed resource allocation and interference management in lte femtocell networks,” in *2013 IEEE 9th International Conference on Wireless and Mobile Computing, Networking and Communications (WiMob)*, 2013, pp. 553–558.
- [29] N. Fath, I. W. Mustika, Selo, K. Yamamoto, and H. Murata, “Optimal resource allocation scheme in femtocell networks based on bat algorithm,” in *2016 22nd Asia-Pacific Conference on Communications (APCC)*, 2016, pp. 281–285.
- [30] M. A. Kamal, H. W. Raza, M. M. Alam, and M. Mazliham, “Resource allocation schemes for 5g network: A systematic review,” 2021.
- [31] M. S. Alomari, A. Ramli, A. Sali, and r. s. a. raja abdullah, “A femtocell cross-tier interference mitigation technique in ofdma-lte system: A cuckoo search based approach,” *Indian Journal of Science and Technology*, vol. 9, 01 2016.
- [32] G. Chen, J. Zheng, and L. Shen, “A preset threshold based cross-tier handover algorithm for uplink co-channel interference mitigation in two-tier femtocell networks,” in *2013 IEEE Global Communications Conference (GLOBECOM)*, 2013, pp. 4717–4722.
- [33] M. Susanto, D. Fauzia, Melvi, and S. Alam, “Downlink power control for interference management in femtocell-macrocell cellular communication network,” in *2017 15th International Conference on Quality in Research (QIR) : International Symposium on Electrical and Computer Engineering*, 2017, pp. 479–484.
- [34] T. Hassan and F. Gao, “An active power control technique for downlink interference management in a two-tier macro-femto network,” *Sensors*, vol. 19, p. 2015, 04 2019.
- [35] M. Osama, S. El Ramly, and B. Abdelhamid, “Interference mitigation and power minimization in 5g heterogeneous networks,” *Electronics*, vol. 10, no. 14, p. 1723, 2021.
- [36] O. I. Ladipo and A. O. Gbenga-Ilori, “Hierarchical power control model for interference mitigation in a two – tier heterogeneous network,” *Cogent Engineering*, vol. 6, no. 1, p. 1691358, 2019.
- [37] Y. Chen, “Mathematical modelling of end-to-end packet delay in multi-hop wireless networks and their applications to qos provisioning,” Nov 2013. [Online]. Available: <https://discovery.ucl.ac.uk/1415093/>
- [38] B. M. Parker, S. Gilmour, J. Schormans, and H. Maruri-Aguilar, “Optimal design of measurements on queueing systems,” *Queueing Syst* 79, pp. 365–390, 2015.
- [39] M. Roshan, J. A. Schormans, and R. Ogilvie, “Video-on-demand qoe evaluation across different age- groups and its significance for network capacity,” *EAI Endorsed Transactions on Mobile Communications and Applications*, vol. 4, no. 12, 1 2018.
- [40] A. Wahab, N. Ahmad, and J. Schormans, “Statistical error propagation affecting the quality of experience evaluation in video on demand applications,” *Applied Sciences*, vol. 10, no. 10, 2020. [Online]. Available: <https://www.mdpi.com/2076-3417/10/10/3662>
- [41] “O-ran alliance.” [Online]. Available: <https://www.o-ran.org/>
- [42] L. M. P. Larsen, A. Checko, and H. L. Christiansen, “A survey of the functional splits proposed for 5g mobile crosshaul networks,” *IEEE Communications Surveys Tutorials*, vol. 21, no. 1, pp. 146–172, 2019.
- [43] B. Balasubramanian, E. S. Daniels, M. Hiltunen, R. Jana, K. Joshi, R. Sivaraj, T. X. Tran, and C. Wang, “Ric: A ran intelligent controller platform for ai-enabled cellular networks,” *IEEE Internet Computing*, vol. 25, no. 2, pp. 7–17, 2021.
- [44] D. Anand, M. A. Togou, and G.-M. Muntean, “A machine learning solution for automatic network selection to enhance quality of service for video delivery,” in *2021 IEEE International Symposium on Broadband Multimedia Systems and Broadcasting (BMSB)*, 2021, pp. 1–5.
- [45] T. J. D. Berstad, M. Riegler, H. Espeland, T. de Lange, P. H. Smedsrud, K. Pogorelov, H. Kvale Stensland, and P. Halvorsen, “Tradeoffs using binary and multiclass neural network classification for medical multidisease detection,” in *2018 IEEE International Symposium on Multimedia (ISM)*, 2018, pp. 1–8.
- [46] O. Owoyele, P. Pal, A. V. Torreira, D. Probst, M. Shaxted, M. Wilde, and P. K. Senecal, “Application of an automated machine learning-genetic algorithm (automl-ga) coupled with computational fluid dynamics simulations for rapid engine design optimization,” 2021. [Online]. Available: <https://arxiv.org/abs/2101.02653>
- [47] R. Medar, V. S. Rajpurohit, and B. Rashmi, “Impact of training and testing data splits on accuracy of time series forecasting in machine learning,” in *2017 International Conference on Computing, Communication, Control and Automation (ICCCUBEA)*, 2017, pp. 1–6.
- [48] M. A. Cano Lengua and E. A. Papa Quiroz, “A systematic literature review on support vector machines applied to classification,” in *2020 IEEE Engineering International Research Conference (EIRCON)*, 2020, pp. 1–4.
- [49] M. Chen, U. Challita, W. Saad, C. Yin, and M. Debbah, “Artificial neural networks-based machine learning for wireless networks: A tutorial,” *IEEE Comms. Surveys & Tutorials*, vol. 21, no. 4, pp. 3039–3071, 2019.
- [50] L. Yang and A. Shami, “On hyperparameter optimization of machine learning algorithms: Theory and practice,” *Neurocomputing*, vol. 415, pp. 295–316, nov 2020. [Online]. Available: